ERJ open research
THE BEST IN OPEN ACCESS BASIC, TRANSLATIONAL & CLINICAL RESPIRATORY RESEARCH

Early View

Original article

Microarray analysis identifies defect in regenerative and immune response pathways in COPD airway basal cells

Fanny Pineau, Gabriella Shumyatsky, Nicole Owuor, Nisha Nalamala, Sudhir Kotnala, Sudhir Bolla, Nathaniel Marchetti, Steven Kelsen, Gerard J. Criner, Uma S. Sajjan

Please cite this article as: Pineau F, Shumyatsky G, Owuor N, *et al*. Microarray analysis identifies defect in regenerative and immune response pathways in COPD airway basal cells. *ERJ Open Res* 2020; in press (https://doi.org/10.1183/23120541.00656-2020).

Microarray analysis identifies defect in regenerative and immune response pathways in COPD airway basal cells

Fanny Pineau[1], Gabriella Shumyatsky[1], Nicole Owuor[1], Nisha Nalamala[1], Sudhir Kotnala[1], Sudhir Bolla[1], Nathaniel Marchetti[1], Steven Kelsen[1], Gerard J Criner[1], Uma S Sajjan[1,2*]

[1]Department of Thoracic Surgery and Medicine and [2]Department of Physiology, Lewis Katz Medical School, Temple University, Philadelphia, PA.

[*] Correspondence should be addressed to Uma Sajjan, Ph.D., Temple University, 3500 N Broad Street, Philadelphia, PA 19140. Phone: (215) 707-7139; Fax: (215) 707-4743; E-mail: uma.sajjan@temple.edu

Short title: Microarray analysis of bronchial basal cells

Grant Support: This work was supported by NIH grants AT007620

Abstract

Background: Airway basal cells are specialized stem cells and regenerate airway epithelium. Airway basal cells isolated from patients with chronic obstructive pulmonary disease (COPD) regenerate airway epithelium with an abnormal phenotype. We performed gene expression analysis to gain insights into the defective regenerative program in COPD basal cells.

Methods: We conducted microarray analysis and compared COPD versus normal basal cells to identify differentially regulated genes (DEG) and the enriched biological pathways. We determined the correlation of DEG with cell polarization and markers of ciliated and goblet cells. HOXB2 was knocked down in 16HBE14o- cells and monitored for polarization of cells. HOXB2 expression in the lung sections was determined by immunofluorescence.

Results: Comparison of normal and COPD basal cell transcriptomic profiles highlighted downregulation of genes associated with tissue development, epithelial cell differentiation and antimicrobial humoral response. Expression of one of the tissue development genes, HOXB2 showed strong correlation with transepithelial resistance and this gene was downregulated in COPD basal cells. Knockdown of HOXB2, abrogated polarization of epithelial cells in normal cells. Finally, HOXB2 expression was substantially reduced in the bronchial epithelium of COPD patients.

Conclusions: Defect in gene signatures involved in tissue development and epithelial differentiation were implicated in COPD basal cells. One of the tissue developmental genes, HOXB2, is substantially reduced in bronchial epithelium of COPD patients. Since HOXB2 contributes to airway epithelial cell polarization, we speculate that reduced expression of HOXB2 in COPD may contribute to abnormal airway epithelial regeneration in COPD.

Introduction

Epithelium lining the conductive airways protects the lungs from environmental factors. In the presence of chronic damage due to persistent inflammation and infection, the protective mechanisms of airway epithelium can malfunction, and this can contribute to the pathology of chronic lung diseases, including chronic obstructive pulmonary disease (COPD). A significant component of dysfunction in these chronic airway diseases is associated with impaired epithelial repair leading to remodeled airway epithelium, inflammation and fibrosis [**1-3**].

COPD is a progressive lung disorder characterized by airflow obstruction. Emphysema, inflammation of large and small airways, mucociliary dysfunction and airway remodeling are common features of COPD [**4, 5**]. Bronchial epithelium in COPD patients often shows basal cell hyperplasia, squamous metaplasia and goblet cell metaplasia.

The basal cells are specialized stem cells present in the tracheobronchial tree and regenerate the conductive airway epithelium following injury. Previously, we and others have demonstrated that basal cells isolated from COPD patients regenerate structurally altered airway epithelium with basal cell hyperplasia and goblet cell metaplasia [**6-9**]. Furthermore, regenerated airway epithelium from COPD basal cells show pro-inflammatory phenotype and reduction in barrier function [**10, 11**]. Now there is compelling evidence that basal cells play a pivotal role in the early pathogenesis of COPD [**9, 12-14**]. Therefore, it is necessary to understand the mechanisms of regenerative pathways that are defective in COPD basal cells.

Comparison of transcriptomic profiles of airway epithelial cells from healthy non-smokers and healthy smokers (with normal lung function and chest imaging) identified 676 differentially expressed genes, primarily upregulated in smokers, and related to development, metabolism, signal transduction, transcription and transport [**15**], with an enrichment of

differentially expressed genes in the chromosomal subband 19q13.2, a COPD risk locus [**16**]. Paradoxically, NOTCH and WNT signaling pathways which were demonstrated to promote goblet cell metaplasia and inflammatory phenotype does not appear to play a role in COPD, because these genes are down-regulated in the airways of these patients [**8, 17-20**]. Transcriptome analysis of airway epithelial cells isolated from bronchioles showed loss of regional transcriptome identity leading to proximalization in smokers with COPD [**21**]. Further, the authors demonstrated that these changes were related to cigarette smoking. However, these findings do not explain the mechanisms underlying the goblet or basal cell hyperplasia observed in the large airways of COPD patients.

In an attempt to gain insight into what influences abnormal differentiation of COPD basal cells, we compared transcriptomic profiles of basal cells obtained from bronchial tissue of healthy never smokers and COPD subjects (who had stopped smoking for at least one year at the time of tissue collection). We also cultured the basal cells at air-liquid interface to determine whether differentially regulated genes (DEG) in basal cells correlates with polarization and differentiation markers. We also examined the functional role of one of the DEG, catergorized under tissue development for its functional role in airway epithelial regeneration.

Materials and methods

Airway epithelial cells

Basal cells were isolated from bronchial segments of normal donor lungs and explanted lungs from COPD patients at the time of lung transplantation as described previously [**7, 8**]. Collection of the tissue was approved by Institutional Review Board of University Michigan, Ann Arbor, MI and Temple University, Philadelphia. Patient characteristics are provided in Supplemental 1**.** The nerve growth factor receptor positive (NGFR+) basal cells were cultured in 12 mm transwells, as described previously [**8, 22**] and harvested either when the basal cells were at 80% confluent or 1, 2 or 4 weeks of culturing at air/liquid interface (ALI).

Microarray and Gene Ontology

Biotinylated cDNAs synthesized from total RNA were subjected to microarray analysis using Human Gene 2.1 ST arrays. at 48°C. The LIMMA methodology (Linear Models for Microarray Data) was applied to the $\log_2$-transformed expression data to identify statistically significant DEG (p-value of < 0.05 and up/down regulated by more than 2-fold) for each comparison and further analyzed. Normalized data and raw data are available in Gene Expression Omnibus (GEO) with accession number GSE137557.

Gene Ontology (GO) and KEGG pathways were analyzed with WebGestalt (WEB-based GEne SeT AnaLysis Toolkit) [**23**] using the Benjamini-Hochberg correction for multiple testing (FDR 5%). For Gene Ontology, only Biological Process terms are discussed because Cellular Component and Molecular Function terms were less relevant.

Flow cytometry

Mucociliary-differentiated cells were dissociated with accutase (ThermoFisher Scientific, Waltham. MA), cells were permeabilized with 4% paraformaldehyde, and incubated in PBS

containing 1% BSA and 0.5% saponin. Cells were then incubated with acetylated tubulin (Sigma Aldrich, St. louis, MO), Muc5AC (Abcam, Cambridge, MA) or TP63 (Abcam), bound antibodies were detected by using Alexafluor-labeled second antibodies. The cells were then analyzed in FACSCalibur Flow cytometer (BD Biosciences, San Jose, CA), and data analyzed by FlowJO version 10 (Tree Star, Ashland, OR).

Transepithelial resistance and Histology

Transepithelial resistance (TER) of airway epithelial cell cultures cultured at ALI for two weeks was determined by using EVOM volt/Ohm meter with EndOhm chambers (World precision Instruments, Sarasota, FL). For histological evaluation, cell cultures were fixed in buffered formalin, embedded in paraffin, 5 μ thick sections were deparaffinized and stained with hematoxylin and eosin (H and E) or periodic acid Schiff's (PAS) reagent.

Real-time PCR

cDNA was synthesized from total RNA and subjected to qPCR to determine the expression of *ADAMTSL3*, *ELF5*, *HOXA1*, *HOXB2*, *IVL*, *KRTDAP*, *STC2*, *ELF5*, and *VGLL1* using a gene-specific primers and probes. The expression levels of each gene is presented as fold change over house-keeping gene, glyceraldehyde 3-phosphate dehydrogenase (*GAPDH*).

Transfection of 16HBE14o- cells

The 16HBE14o- cells (immortalized bronchial epithelial cell line) were transfected with smart pool HOXB2 siRNA or non-targeting siRNA (Horizon Discovery, Lafayette, CO), as described previously [**24**]. TER was measured 48h after transfection to assess polarization of cells.

Immunofluorescence staining.

Cells growing in transwells were fixed, permeabilized, blocked and incubated with antibody to E-cadherin or occludin. The bound antibodies were detected with appropriate Alexafluor-labeled antibodies, counter stained with DAPI and imaged by using Zeiss confocal microscope [**25**]. Lung tissue at second and third branching of bronchi was collected from 6 COPD and 6 healthy non-smokers under the approval of Temple Institute Review Board. The tissues were fixed in 10% buffered formaldehyde, embedded in paraffin and 5 μ thick sections were used for detection of HOXB2 by immunofluorescence microscopy using antibody from Developmental Studies Hybridoma Bank, University of Iowa, Iowa City, IA and tyramide signal amplification method.

Western blot analysis

Total protein from cells was subjected to Western blot analysis with antibodies to E-cadherin, occludin, HOXB2 and β-actin. Density of the protein bands was determined by ImageJ and expressed as fold increase over β-actin.

Statistical analysis

Data are presented as median with range. Statistical significance was assessed by non-parametric analysis, Mann-Whitney test to compare two groups and ANOVA on Ranks with Kruskal Wallace non parametric test to compare three groups. A p-value of ≤ 0.05 was considered as statistically significant.

Results

Phenotypic characterization of airway epithelium regenerated from basal cells isolated from normal and COPD subjects

As previously observed basal cells from both normal and COPD subjects regenerated mucociliary-differentiated airway epithelium (Figure 1A), with COPD cell cultures showing

more goblet cells as assessed by PAS staining (Figure 1B) [**7, 8**]. Quantification of cell types by flow cytometry showed significantly more goblet cells and basal cells and less ciliated cells in COPD than in normal (Figure 1C). Normal cultures polarize by two weeks of culturing at air/liquid interface, and polarization of cells is necessary for the differentiation of cells. Therefore, we determined the TER at two weeks of culturing at air/liquid interface, and COPD cell cultures showed significantly lower TER than normal cultures (Figure 1D). To identify the possible biological pathways that lead to defective airway epithelial regeneration, we conducted transcriptome analysis on COPD and normal basal and differentiated airway epithelial cell cultures.

Differentially expressed genes between COPD and normal basal cells

To determine a COPD-specific transcriptomic signature, we compared basal cells from COPD (C) and healthy subjects (N). In this analysis, 99 probes showed differential expression (30 upregulated, 69 downregulated in COPD), and 70 of them mapped to known transcripts (Figure 2A and Supplementary Table 2). The most differentially expressed genes (DEG) included *HOXA1*, *HIST3H2BB*, *TENM2*, *SLC2A12*, *VGLL1*, *ARHGAP40* and *HOXB2* (Table 1). Gene Ontology (GO) analysis of the DEG showed an overrepresentation among genes associated with epithelial/epidermal cell differentiation, cornification, and antimicrobial humoral response (Supplemental Table 3). All genes in these GO categories were downregulated in COPD cells. Genes involved in epithelial/epidermal cell differentiation and cornification, and tissue development categories included genes encoding kallikreins, keratins, S100 calcium binding protein A7 (S100A7), desmoglein 1 (DSG1), uroplakin 1A (UPK1A), E74-like factor 5 (ELF5), *HOXB2*, *VGLL1* and *KRTDAP* (Table 1).

Table 1: Expression data for top up- and downregulated genes in COPD compared to normal basal cells and genes involved in epithelial/epidermal differentiation and tissue development

Gene	**C avg**	±SD	**N avg**	±SD	**Fold**	**p-value**

Symbol	(log2)		(log2)		Change	
Top-20 downregulated genes in COPD						
HOXA1	1.51	0.70	3.67	0.50	-4.47	1.8E-06
TENM2	6.98	0.45	8.13	0.28	-2.21	3.3E-06
SLC2A12	2.93	0.57	4.61	0.65	-3.19	2.0E-05
VGLL1	5.06	0.61	6.67	0.57	-3.05	4.7E-05
ARHGAP40	1.75	0.51	3.21	0.72	-2.76	1.0E-04
CLIC3	5.23	0.59	6.48	0.66	-2.38	2.0E-04
HOXB2	1.89	0.31	3.29	0.93	-2.64	2.0E-04
IL36RN	2.76	0.45	3.76	0.69	-2.00	3.0E-04
PADI1	3.31	0.63	4.76	0.76	-2.73	5.0E-04
MFAP5	4.49	0.68	6.31	0.85	-3.53	5.0E-04
ATP12A	5.06	1.26	7.23	1.40	-4.48	8.0E-04
FAM46C	2.21	0.40	3.23	0.60	-2.02	9.0E-04
MAL	4.20	0.73	6.31	1.75	-4.32	1.0E-03
KLK5	4.47	0.77	5.90	0.84	-2.68	1.1E-03
HEPHL1	1.25	0.31	2.59	1.16	-2.53	1.1E-03
LGALS9B	4.86	0.62	6.43	0.79	-2.97	1.2E-03
ELF5	3.84	0.57	4.92	0.93	-2.12	2.2E-03
KLK7	7.42	0.50	8.45	0.93	-2.05	2.4E-03
SCNN1G	3.45	0.72	4.65	0.60	-2.31	2.7E-03
UPK1A	1.96	0.55	3.94	1.93	-3.96	2.8E-03
IVL	3.92	1.03	5.1	1.1	-2.27	0.0093
KRTDAP	2.47	0.6	3.59	1.57	-2.17	0.0114
S100A7	1.82	0.89	3.17	1.18	-2.55	0.0186
KRT24	1.66	0.94	3.28	1.15	-3.06	0.0241
DSG1	2.64	1.65	4.32	1.96	-3.21	0.0411
Top-10 upregulated genes in COPD						
HIST3H2BB	4.92	0.41	3.78	0.38	2.21	2.1E-06
CLGN	3.83	0.80	2.19	0.50	3.12	3.0E-04
HIST1H3J	5.33	0.44	4.08	0.58	2.39	3.0E-04
HIST1H2AB	6.02	0.61	4.51	0.51	2.84	4.0E-04
ANXA10	6.24	1.33	4.24	1.16	3.99	4.0E-03
HIST1H3H	2.70	0.26	1.62	0.83	2.13	6.0E-03
CHAC1	6.73	1.32	4.83	0.45	3.72	1.2E-02
CCNE2	5.67	0.75	4.62	0.29	2.07	1.6E-02
GTF2H2	1.75	1.09	0.65	0.62	2.15	3.3E-02
ADAMTSL3	4.25	0.95	3.15	0.84	2.14	3.6E-02
Control genes						
GAPDH	4.11	2.11	4.21	0.12	-1.07	0.2273
KRT5	10.13	0.12	10.36	0.17	-1.10	0.0155

Highlighted in green, genes involved in tissue development
Highlighted in yellow, genes involved in epithelial/epidermal differentiation

Validation of DEG between COPD and normal basal cells using RT-PCR

To confirm the differences observed between COPD and normal basal cells in microarray analysis, we measured the expression levels of some of the DEG involved in either epithelial differentiation or tissue development, and STC2 and ADAMTSL3, which are not involved in either of these categories using probe-based qPCR. *HOXA1*, *HOXB2*, *STC2*, *ELF5* and *VGLL1* showed significant differences between normal and COPD; *ADAMTSL3*, *KRTDAP* and *IVL* showed changes in the same direction as observed with microarray though differences were not significant (Figure 2B-2I).

Correlation of tissue development and epithelial differentiation with phenotypic features of differentiated cultures

Next, we evaluated whether DEG associated with tissue development/epithelial differentiation categories correlate with polarization or differentiation. The cells cultured at air/liquid interface from the same batch of basal cells used in the microarray analysis were used for this analysis. TER measured at 2 weeks of culturing at ALI, and mRNA expression of FOXJ1 (marker of ciliated cells) and MUC5AC (marker of goblet cells) was determined at 4 weeks of culturing at ALI. Interestingly, mRNA expression of HOXA1 and HOXB2 in basal cells showed strong correlation with polarization of cells (TER), a necessary step for differentiation, but not with differentiation markers MUC5AC (goblet cell marker) or FOXJ1 (ciliated cell marker) (Figure 3A to 3F). ELF5 and KRTDAP on the other hand showed some correlation with TER, MUC5AC and FOXJ1 (Supplemental Figure 1A and 1B). VGLL1 did not correlate with either TER or differentiation markers (Supplemental Figure 1C). Compared to normal, COPD cells also showed lower expression of occludin and E-cadherin, representatives of tight and adherence junction proteins respectively (Figure 4A - 4C). These observations indicate that HOXA1 and HOXB2 may participate in polarization of the cells, which is altered in COPD.

Kinetics of HOXA1 and HOXB2 expression in regenerating airway epithelium

To determine whether HOXA1 and HOXB2 expression changes during the regeneration of airway epithelium, we assessed the expression of these two genes in basal cells and the confluent basal cells cultured at ALI for 1, 2 and 4 weeks. In normal cells, while the expression of HOXA1 remained same throughout the culturing period (Figure 5), the expression of HOXB2 increased with time of culturing showing maximum expression at 2 weeks. In COPD cells, expression of both HOXA1 and HOXB2 showed increasing trend with time of culturing, which did not reach statistical significance. Expression of both genes was significantly lower in COPD than normal cells at all time points.

Since the HOXB2 expression dynamically changed and reached maximum at 2 weeks when the cells polarize, we examined the contribution of HOXB2 in polarization of cells. We used a bronchial epithelial cell line, 16HBE14o-, which polarizes when cultured on semipermeable membrane. We knocked down HOXB2 in 16HBE14o- cells by using gene-specific siRNA and assessed cell polarization by measuring TER, and the expression and localization of occludin and E-cadherin. Compared to non-targeting (NT) siRNA, HOXB2 siRNA-transfected cells showed significantly lower TER (Figure 6A) and this was associated with attenuated expression of E-cadherin and occludin in the apicolateral junctions of the cells (Figure 6B and 6C). Western blot analysis indicated reduced expression of both occludin and E-cadherin (Figure 6D to 6F). Successful knockdown of HOXB2 was confirmed by Western blot analysis (Figure 6G).

Bronchial epithelium in COPD lungs show reduced expression of HOXB2.

Immunofluorescence microscopy was performed to examine the expression of HOXB2 in the second and third branching of bronchi in normal and COPD lung sections. The HOXB2 expression was observed in the bronchial epithelium of both normal and COPD lungs (Figure

7A and 7B), but it was substantially lower in COPD than in normal. Expression of HOXB2 was primarily observe din the nuclei of all the cells in the bronchial epithelium. Isotype IgG control showed no signals indicating the specificity of the HOXB2 antibody (Figure 7C).

Taken together these results indicate that COPD and normal basal cells show significant differences in the expression of certain genes which are involved in tissue development and epithelial/epidermal differentiation. Our studies also indicate that HOXB2 may contribute to polarization of bronchial epithelial cells.

Discussion

Airway epithelium from COPD show abnormal phenotype and this may be due to altered gene expression in basal cells, which play a fundamental role in regenerating the epithelium [**13, 14**]. To identify altered regenerative mechanisms and pathways in airway basal cells in COPD, we determined gene expression levels in COPD and normal basal cells by using microarrays. We then confirmed the contribution of one of the developmental genes, HOXB2 in polarization of cells, which is a necessary step during epithelial regeneration. We also demonstrate that HOXB2 is not only reduced in COPD cells *in vitro*, but also in the bronchial epithelium of COPD patients.

Comparing transcriptomic profiles of basal cells from COPD and normal subjects, we identified a COPD-specific signature. Genes associated with tissue development, epithelial cell differentiation were underrepresented in COPD basal cells, indicating that regenerating programs are altered in these cells. Out of the four genes identified under the tissue development category, HOXA1 and HOXB2 are expressed in adult human lungs and the expression is reduced in emphysematous lungs [**30**], but their role in regeneration of airway epithelium has never been studied. The present study demonstrates that HOXB2 expression is substantially reduced in the bronchial epithelium of COPD patients compared to normal

subjects. Furthermore, HOXB2 expression dynamically changes reaching maximum at the time of cell polarization during the regeneration of normal epithelium *in vitro* indicating HOXB2 may contribute to cell polarization. Consistent with this notion, knockdown of HOXB2 led to reduction in TER and this was associated with reduced expression of E-cadherin and occludin. Further studies are needed to evaluate the mechanisms underlying the regulation of adherence and tight junction proteins by HOXB2.

Microarray analysis also identified reduced expression of desmoglein (DSG)1 and actin binding LIM (*ABLIM)3* in COPD cells. *DSG1*, a major component of intercellular desmosome junctions is involved in the interaction of plaque proteins and intermediate filaments mediating cell-cell adhesion. *ABLIM3*, which interacts with actin filaments and is thought to be a component of adherens junctions [**29**]. Role of HOXB2 in regulating these genes is yet to be determined and will be addressed in the future study.

The cell-differentiation associated DEG included genes encoding cytokeratins (KRT4, 6C, 24), expressed during differentiation of epithelial cells and responsible for their structural integrity; *PADI1, 3*, involved in the late stages of epidermal differentiation; and *ELF5*, member of an epithelium specific subclass of the Ets transcription factor family that is required for proper lung development and differentiation of epithelial cells [**26**]. In the present study, *ELF5* showed correlation with differentiation markers, *MUC5AC* and *FOXJ1* indicating that *ELF5* may contribute bronchial epithelial differentiation. Interestingly, *ELF5* maps to 11p13, a genomic region that has been associated with cystic fibrosis lung disease severity in genome-wide association studies [**27, 28**] and can be considered as a COPD risk locus. Interestingly, three other differentially expressed transcripts in our study mapped to COPD risk loci: *CNFN* in 19q13.2, *SNORD111* in 16q22.1, and *LOC105374160* in 3q25.1 [**15**].

DEG between COPD and normal basal cells also included genes associated with antimicrobial response, all downregulated in COPD: the Peptidoglycan Recognition Proteins 3 and 4 (PGLYRP3, 4) that bind to peptidoglycans of Gram positive and/or negative bacteria, the CXCL14 cytokine that plays chemotactic activity for monocytes and may be involved in the homeostasis of monocyte-derived macrophages, and the interleukin 36 receptor antagonist (IL36RN), member of the IL-1 cytokine family and specifically inhibits the activation of NF-kappaB induced by IL1F6 [**31**]. The Glutathione-specific Gamma-Glutamylcyclotransferase 1 (CHAC1), expression of which was upregulated in COPD basal cells, mediates the ATF4-ATF3-DDIT3/CHOP cascade and acts as a pro-apoptotic component of the unfolded protein response. It also regulates the oxidative balance by catalyzing the cleavage of glutathione. These results indicate that COPD basal cells may acquire epigenomic changes which affects expression of genes that involved in regeneration and maintenance of homeostasis of airway epithelium.

Previously, RNAseq analysis of basal cells from never smokers and active smokers identified 676 smoking-dysregulated genes [**15**], but there was no overlap between these genes and the dysregulated genes that were identified in the present study. These observations indicate that the dysregulated genes identified in this study may be specific to end-stage COPD disease, because all the basal cells were obtained during lung transplantation. Moreover, our patients had stopped smoking at least for 6 months prior to surgery, therefore we may have lost the changes in gene expression that occur during active smoking. It would be interesting to compare the transcriptomic profiles generated from former-smoker COPD patients with the ones of active-smoker COPD patients. This requires prospective collection of the tissue which we plan to conduct in the near future.

In summary, basal cells from COPD patients show downregulation of genes associated with epithelial cell differentiation, cell junctions, dysregulation of focal adhesion pathways, all of

which may contribute to regeneration of abnormal airway epithelium. HOXB2, one of the downregulated genes in COPD basal cells was found to contribute to polarization of cells. Finally, compared to normal, COPD bronchial epithelium showed reduced of HOXB2 protein. These studies provide valuable information for future investigations on the contribution of dysregulated genes in epithelial regeneration and immune responses in COPD.

Acknowledgments

We thank Dr. Fernando Martinez, Cornell University, Ithaca, NY and Dr. Catherine Meldrum, University of Michigan, Ann Arbor, MI for helping us to obtain tracheobronchial segments from healthy and COPD subjects. We also thank Biobank facility of the Lung center, Temple University for providing lung tissue samples for preparing paraffin blocks. We thank Microarray core facility at University of Michigan for performing microarrays on normal and COPD samples and assistance with preliminary data analysis.

References

1. Ganesan S, Comstock AT, Sajjan US. Barrier function of airway tract epithelium**.** *Tissue Barriers* 2013, **1:**e24997.
2. Beers MF, Morrisey EE. The three R's of lung health and disease: repair, remodeling, and regeneration**.** *J Clin Invest* 2011, **121:**2065-2073.
3. Regamey N, Jeffery PK, Alton EW, Bush A, Davies JC. Airway remodelling and its relationship to inflammation in cystic fibrosis**.** *Thorax* 2011, **66:**624-629.
4. Barnes PJ, Shapiro SD, Pauwels RA. Chronic obstructive pulmonary disease: molecular and cellular mechanisms**.** *Eur Respir J* 2003, **22:**672-688.
5. Decramer M, Janssens W, Miravitlles M. Chronic obstructive pulmonary disease**.** *The Lancet* 2012, **379:**1341-1351.
6. Staudt MR, Buro-Auriemma LJ, Walters MS, Salit J, Vincent T, Shaykhiev R, Mezey JG, Tilley AE, Kaner RJ, Ho MW, Crystal RG. Airway Basal stem/progenitor cells have diminished capacity to regenerate airway epithelium in chronic obstructive pulmonary disease**.** *Am J Respir Crit Care Med* 2014, **190:**955-958.
7. Schneider D, Ganesan S, Comstock AT, Meldrum CA, Mahidhara R, Goldsmith AM, Curtis JL, Martinez FJ, Hershenson MB, Sajjan U. Increased cytokine response of rhinovirus-infected airway epithelial cells in chronic obstructive pulmonary disease**.** *Am J Respir Crit Care Med* 2010, **182:**332-340.
8. Jing Y, Gimenes JA, Mishra R, Pham D, Comstock AT, Yu D, Sajjan U. NOTCH3 contributes to rhinovirus-induced goblet cell hyperplasia in COPD airway epithelial cells**.** *Thorax* 2019, **74:**18-32.
9. Ghosh M, Miller YE, Nakachi I, Kwon JB, Baron AE, Brantley AE, Merrick DT, Franklin WA, Keith RL, Vandivier RW. Exhaustion of Airway Basal Progenitor Cells

in Early and Established Chronic Obstructive Pulmonary Disease**.** *Am J Respir Crit Care Med* 2018, **197:**885-896.

10. Ganesan S, Unger BL, Comstock AT, Angel KA, Mancuso P, Martinez FJ, Sajjan US. Aberrantly activated EGFR contributes to enhanced IL-8 expression in COPD airways epithelial cells via regulation of nuclear FoxO3A**.** *Thorax* 2013, **68:**131-141.
11. Milara J, Peiro T, Serrano A, Cortijo J. Epithelial to mesenchymal transition is increased in patients with COPD and induced by cigarette smoke**.** *Thorax* 2013, **68:**410-420.
12. Randell SH. Airway epithelial stem cells and the pathophysiology of chronic obstructive pulmonary disease**.** *Proc Am Thorac Soc* 2006, **3:**718-725.
13. Crystal RG. Airway basal cells. The "smoking gun" of chronic obstructive pulmonary disease**.** *Am J Respir Crit Care Med* 2014, **190:**1355-1362.
14. Shaykhiev, Crystal. Basal cell origins of smoking induced airway epithelial disorders**.** 2013.
15. Ryan DM, Vincent TL, Salit J, Walters MS, Agosto-Perez F, Shaykhiev R, Strulovici-Barel Y, Downey RJ, Buro-Auriemma LJ, Staudt MR, et al. Smoking dysregulates the human airway basal cell transcriptome at COPD risk locus 19q13.2**.** *PLoS One* 2014, **9:**e88051.
16. Cho MH, Castaldi PJ, Wan ES, Siedlinski M, Hersh CP, Demeo DL, Himes BE, Sylvia JS, Klanderman BJ, Ziniti JP, et al. A genome-wide association study of COPD identifies a susceptibility locus on chromosome 19q13**.** *Hum Mol Genet* 2012, **21:**947-957.
17. Rock JR, Gao X, Xue Y, Randell SH, Kong YY, Hogan BL. Notch-dependent differentiation of adult airway basal stem cells**.** *Cell Stem Cell* 2011, **8:**639-648.

18. Gomi K, Arbelaez V, Crystal RG, Walters MS. Activation of NOTCH1 or NOTCH3 signaling skews human airway basal cell differentiation toward a secretory pathway**.** *PLoS One* 2015, **10:**e0116507.

19. Wang R, Ahmed J, Wang G, Hassan I, Strulovici-Barel Y, Hackett NR, Crystal RG. Down-regulation of the canonical Wnt beta-catenin pathway in the airway epithelium of healthy smokers and smokers with COPD**.** *PLoS One* 2011, **6:**e14793.

20. Danahay H, Pessotti AD, Coote J, Montgomery BE, Xia D, Wilson A, Yang H, Wang Z, Bevan L, Thomas C, et al. Notch2 is required for inflammatory cytokine-driven goblet cell metaplasia in the lung**.** *Cell Rep* 2015, **10:**239-252.

21. Yang J, Zuo WL, Fukui T, Chao I, Gomi K, Lee B, Staudt MR, Kaner RJ, Strulovici-Barel Y, Salit J, et al. Smoking-Dependent Distal-to-Proximal Repatterning of the Adult Human Small Airway Epithelium**.** *Am J Respir Crit Care Med* 2017, **196:**340-352.

22. Ganesan S, Pham D, Jing Y, Farazuddin M, Hudy MH, Unger B, Comstock AT, Proud D, Lauring AS, Sajjan US. TLR2 Activation Limits Rhinovirus-Stimulated CXCL-10 by Attenuating IRAK-1-Dependent IL-33 Receptor Signaling in Human Bronchial Epithelial Cells**.** *J Immunol* 2016, **197:**2409-2420.

23. Wang J, Vasaikar S, Shi Z, Greer M, Zhang B. WebGestalt 2017: a more comprehensive, powerful, flexible and interactive gene set enrichment analysis toolkit**.** *Nucleic Acids Res* 2017, **45:**W130-W137.

24. Unger BL, Ganesan S, Comstock AT, Faris AN, Hershenson MB, Sajjan US. Nod-like receptor X-1 is required for rhinovirus-induced barrier dysfunction in airway epithelial cells**.** *J Virol* 2014, **88:**3705-3718.

25. Faris AN, Ganesan S, Chattoraj A, Chattoraj SS, Comstock AT, Unger BL, Hershenson MB, Sajjan US. Rhinovirus Delays Cell Repolarization in a Model of

Injured/Regenerating Human Airway Epithelium**.** *Am J Respir Cell Mol Biol* 2016, **55:**487-499.

26. Metzger DE, Stahlman MT, Shannon JM. Misexpression of ELF5 disrupts lung branching and inhibits epithelial differentiation**.** *Dev Biol* 2008, **320:**149-160.

27. Wright FA, Strug LJ, Doshi VK, Commander CW, Blackman SM, Sun L, Berthiaume Y, Cutler D, Cojocaru A, Collaco JM, et al. Genome-wide association and linkage identify modifier loci of lung disease severity in cystic fibrosis at 11p13 and 20q13.2**.** *Nat Genet* 2011, **43:**539-546.

28. Stolzenburg LR, Yang R, Kerschner JL, Fossum S, Xu M, Hoffmann A, Lamar KM, Ghosh S, Wachtel S, Leir SH, Harris A. Regulatory dynamics of 11p13 suggest a role for EHF in modifying CF lung disease severity**.** *Nucleic Acids Res* 2017, **45:**8773-8784.

29. Matsuda M, Yamashita JK, Tsukita S, Furuse M. abLIM3 is a novel component of adherens junctions with actin-binding activity**.** *Eur J Cell Biol* 2010, **89:**807-816.

30. Golpon HA, Geraci MW, Moore MD, Miller HL, Miller GJ, Tuder RM, Voelkel NF. HOX genes in human lung: altered expression in primary pulmonary hypertension and emphysema**.** *Am J Pathol* 2001, **158:**955-966.

31. Debets R, Timans JC, Homey B, Zurawski S, Sana TR, Lo S, Wagner J, Edwards G, Clifford T, Menon S, et al. Two novel IL-1 family members, IL-1 delta and IL-1 epsilon, function as an antagonist and agonist of NF-kappa B activation through the orphan IL-1 receptor-related protein 2**.** *J Immunol* 2001, **167:**1440-1446.

32. Amatngalim GD, Schrumpf JA, Henic A, Dronkers E, Verhoosel RM, Ordonez SR, Haagsman HP, Fuentes ME, Sridhar S, Aarbiou J, et al. Antibacterial Defense of Human Airway Epithelial Cells from Chronic Obstructive Pulmonary Disease Patients

Induced by Acute Exposure to Nontypeable Haemophilus influenzae: Modulation by Cigarette Smoke**.** *J Innate Immun* 2017, **9:**359-374.

33. Schmid A, Sailland J, Novak L, Baumlin N, Fregien N, Salathe M. Modulation of Wnt signaling is essential for the differentiation of ciliated epithelial cells in human airways**.** *FEBS Lett* 2017, **591:**3493-3506.

34. Malleske DT, Hayes D, Jr., Lallier SW, Hill CL, Reynolds SD. Regulation of Human Airway Epithelial Tissue Stem Cell Differentiation by beta-Catenin, P300, and CBP**.** *Stem Cells* 2018, **36:**1905-1916.

35. Gomi K, Staudt MR, Salit J, Kaner RJ, Heldrich J, Rogalski AM, Arbelaez V, Crystal RG, Walters MS. JAG1-Mediated Notch Signaling Regulates Secretory Cell Differentiation of the Human Airway Epithelium**.** *Stem Cell Rev Rep* 2016, **12:**454-463.

36. Golebski K, van Egmond D, de Groot EJ, Roschmann KI, Fokkens WJ, van Drunen CM. EGR-1 and DUSP-1 are important negative regulators of pro-allergic responses in airway epithelium**.** *Mol Immunol* 2015, **65:**43-50.

37. Kramer EL, Mushaben EM, Pastura PA, Acciani TH, Deutsch GH, Khurana Hershey GK, Korfhagen TR, Hardie WD, Whitsett JA, Le Cras TD. Early growth response-1 suppresses epidermal growth factor receptor-mediated airway hyperresponsiveness and lung remodeling in mice**.** *Am J Respir Cell Mol Biol* 2009, **41:**415-425.

38. Reynolds PR, Cosio MG, Hoidal JR. Cigarette smoke-induced Egr-1 upregulates proinflammatory cytokines in pulmonary epithelial cells**.** *Am J Respir Cell Mol Biol* 2006, **35:**314-319.

Figure legends

Figure 1: Airway epithelium regenerated from COPD basal cells show abnormal phenotype. Basal cells from 8 normal and 8 COPD subjects were cultured in transwells at ALI for 4 weeks. The transwells were transferred to new receiver plates containing fresh medium and incubated for 24 hours prior to harvesting. The cultures in the transwells were fixed in 10% buffered formalin, embedded in paraffin, and the paraffin sections were stained with H & E (A) or PAS (B). Arrow heads in panel A indicate cilia and arrows in panel B indicate goblet cells. Images in A and B are representative of eight COPD and eight normal regenerated airway epithelial cell cultures. From identical cultures, cells were dissociated and subjected to flow cytometry to determine different cell population and data represent mean ± SD (C). TER was measured after culturing basal cells at air/liquid interface for 2 weeks (D). Data represents median and range. The statistical significance was either determined by unpaired t test (C) or by Mann-Whitney nonparametric test (D).

Figure 2. Differentially regulated genes in basal COPD and normal cells. Valcano plot showing differential gene expression between basal cells from 8 COPD and 8 normal subjects (C vs N): (A); Red, down regulated genes; green, upregulated genes. Total RNA isolated from the basal cells was subjected to RT-qPCR (B – I). Data represents median with range form 8 COPD and 8 normal subjects and statistical significance was determined by Mann-Whitney test.

Figure 3. Expression of HOXA1 and HOXB2 in basal cells correlates with TER and not differentiation markers. Basal cells from 8 normal and 8 COPD subjects were cultured at air/liquid interface for 2 (to assess TER) or 4 weeks (to assess MUC5AC and FOXJ1). Total RNA was isolated from basal cells and cells cultured at ALI for 4 weeks. mRNA expression of HOXA1 and HOXB2 in basal cells, and MUC5AC and FOXJ1 were determined by probe-

based qPCR. The data was normalized to GAPDH. TER measured in cells cultured at ALI for 2 weeks correlates with the expression of HOXA1 and HOXB2 (A and D). The expression of either HOXA1 or HOXB2 does not show strong correlation with differentiation markers MUC5AC or FOXJ1 (B, C, E and F). Red and black dots in all the panels represent data from normal and COPD cells respectively.

Figure 4. COPD cells show reduced expression of E-cadherin and occludin proteins. Total protein isolated from polarized cells was subjected to Western blot analysis to determine the protein expression of E-cadherin and occludin (A). Image is representative of 8 normal and 8 COPD subjects. The density of bands were determined and expressed as fold change over β-actin (B and C). The data represent mean ± SD calculated from 8 normal and 8 COPD basal cells from 3 independent experiment and the significance was assessed by unpaired t test.

Figure 5. HOXB2 expression shows dynamic changes during culturing. Total RNA from basal cells and basal cells cultured at ALI for 1, 2, and 4 weeks was isolated, cDNA was synthesized and subject to probe-based qPCR to determine the expression of HOXA1 and HOXB2 (A and B). The data represent median with range. Statistical significance was determined by ANOVA on Ranks with Kruskal Wallace post-hoc test. Numbers in bold represents difference in the expression of genes between normal and COPD cells at each time point. HOXB2 expression significantly changed with time of culturing but not in COPD cells.

Figure 6. HOXB2 contributes to epithelial cell polarization. The 16HBE14o- cells cultured in transwells (90% confluent) were transfected with NT or HOXB2 siRNA and incubated for another 2 days to promote polarization and then TER was measured (A). Cells were fixed to assess the localization of occludin and E-cadherin by immunofluorescene microscopy (B and C). From identical cultures, total protein was isolated and expression of occludin and E-cadherin was determined by Western blot analysis (D). Density of the bands was determined

and expressed as fold change over β-actin (E and F). The data represent mean ± SD calculated from 4 independent experiments and unpaired t test was used to calculate the p value. HOXB2 knockdown was confirmed by Western blot analysis (G). Images in B,C, D and G are representative from 4 independent experiments.

Figure 7. Immunolocalization of HOXB2 in lung tissues. Paraffin sections of COPD and normal lungs were deparaffinized, incubated for 10 min in boiling 10 mM citrate buffer pH 6.0, allowed to cool down to room temperature. The sections were then treated with 3% hydrogen peroxide to quench endogenous peroxidase activity, blocked with 5% normal horse serum containing 0.3% Triton X-100 for 1h. Slides were washed and incubated with primary antibody for 16 h at 4°C. The slides were washed, incubated with tyramide conjugated with AlexaFlour 488 and then counterstained with DAPI. Red, HOXB2 in the left panels, blue, nuclei in the center panels and magenta, colocalization of HOXB2 with nuclei in right panels. A and B. Normal and COPD lung section respectively stained with HOXB2 antibody. C. Normal lung section stained with isotype control IgG. The images are representative of lung sections from 6 normal and 6 COPD subjects.

Figure 1

A

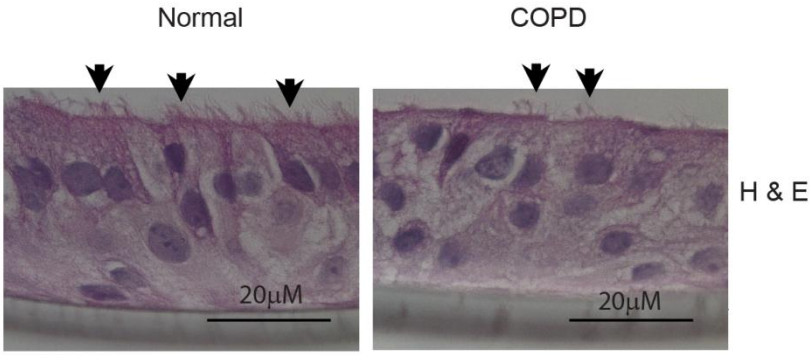

B

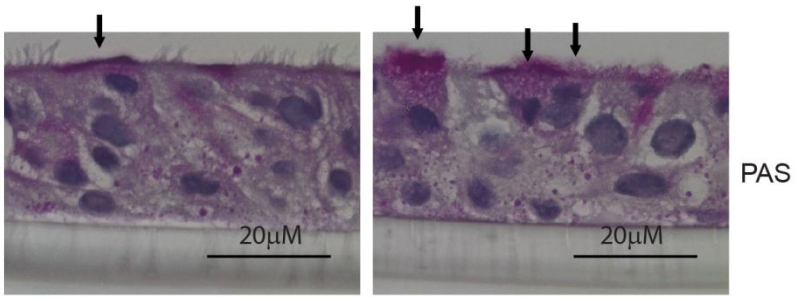

C

Regenerated airway epithelium	TP63+ Basal cells	MUC5AC+ Goblet cells	Acetylated tubulin+ ciliated cells
Normal	24 ± 3.5	16 ± 4.1	41 ± 2.5
COPD	32 ± 2.2*	25 ± 3.6*	30 ± 2.4*

*p=<0.05, unpaired t test

D

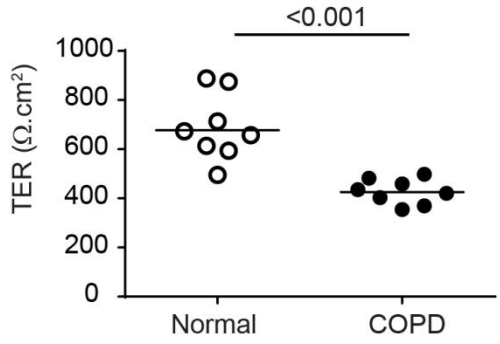

Figure 2

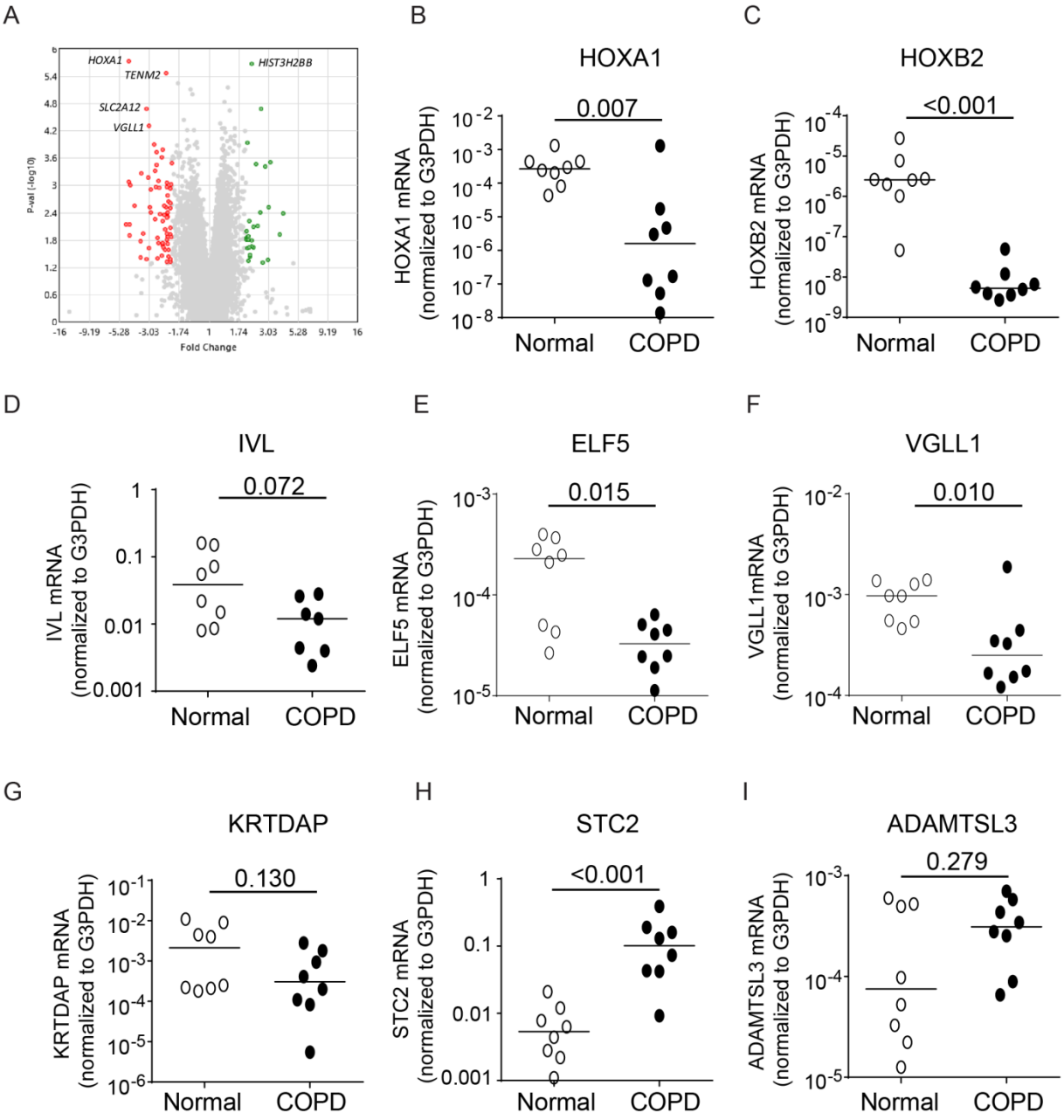
A
HOXA1
TENM2
SLC2A12
VGLL1
HIST3H2BB
P-val (-log10)
Fold Change
B
HOXA1
0.007
HOXA1 mRNA (normalized to G3PDH)
Normal
COPD
C
HOXB2
<0.001
HOXB2 mRNA (normalized to G3PDH)
Normal
COPD
D
IVL
0.072
IVL mRNA (normalized to G3PDH)
Normal
COPD
E
ELF5
0.015
ELF5 mRNA (normalized to G3PDH)
Normal
COPD
F
VGLL1
0.010
VGLL1mRNA (normalized to G3PDH)
Normal
COPD
G
KRTDAP
0.130
KRTDAP mRNA (normalized to G3PDH)
Normal
COPD
H
STC2
<0.001
STC2 mRNA (normalized to G3PDH)
Normal
COPD
I
ADAMTSL3
0.279
ADAMTSL3 mRNA (normalized to G3PDH)
Normal
COPD

Figure 3

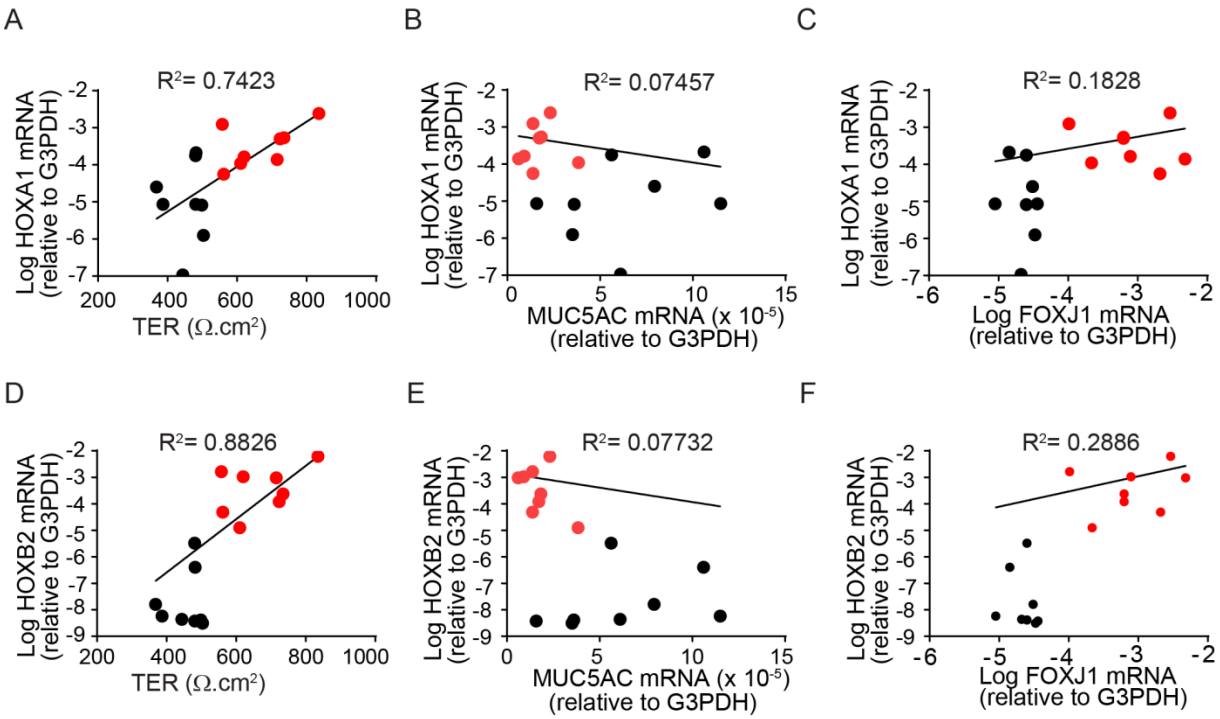
A
B
C
D
E
F
R²= 0.7423
R²= 0.07457
R²= 0.1828
R²= 0.8826
R²= 0.07732
R²= 0.2886
Log HOXA1 mRNA (relative to G3PDH)
Log HOXB2 mRNA (relative to G3PDH)
TER (Ω.cm²)
MUC5AC mRNA (x 10⁻⁵) (relative to G3PDH)
Log FOXJ1 mRNA (relative to G3PDH)

Figure 4

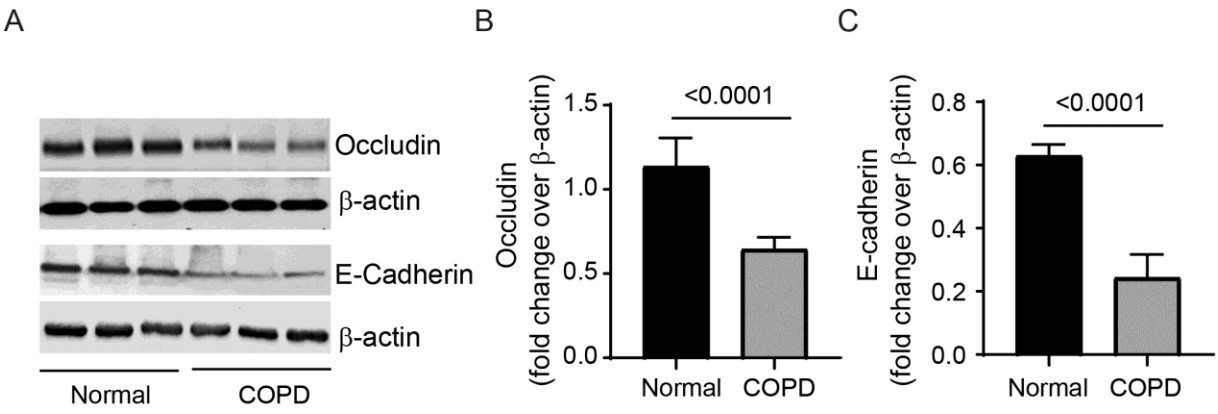
A
Occludin
β-actin
E-Cadherin
β-actin
Normal
COPD
B
Occludin (fold change over β-actin)
1.5
1.0
0.5
0.0
<0.0001
Normal
COPD
C
E-cadherin (fold change over β-actin)
0.8
0.6
0.4
0.2
0.0
<0.0001
Normal
COPD

Figure 5

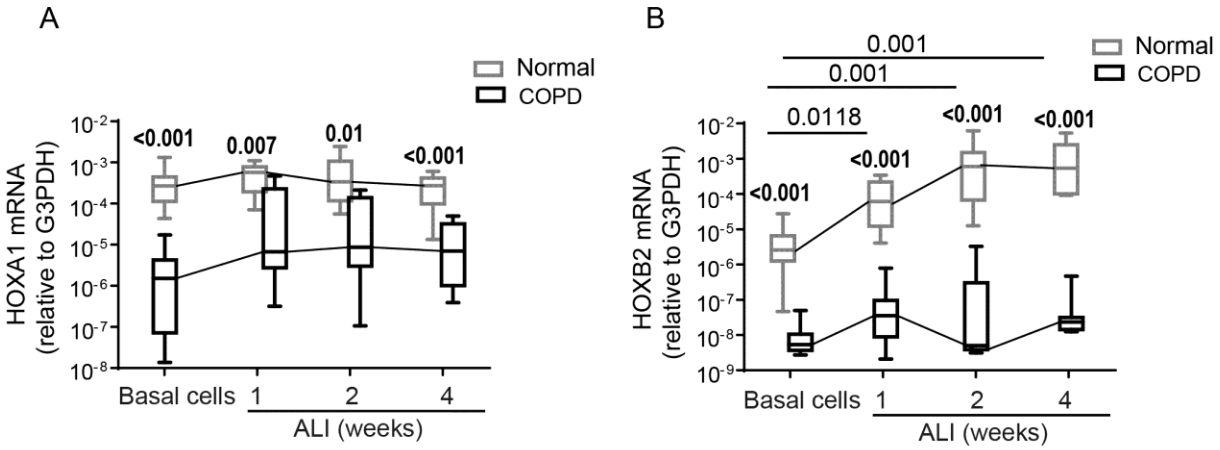
A
Normal
COPD
HOXA1 mRNA (relative to G3PDH)
<0.001
0.007
0.01
<0.001
Basal cells
1
2
4
ALI (weeks)
B
0.001
0.001
0.0118
<0.001
<0.001
<0.001
HOXB2 mRNA (relative to G3PDH)
Basal cells
1
2
4
ALI (weeks)

Figure 6

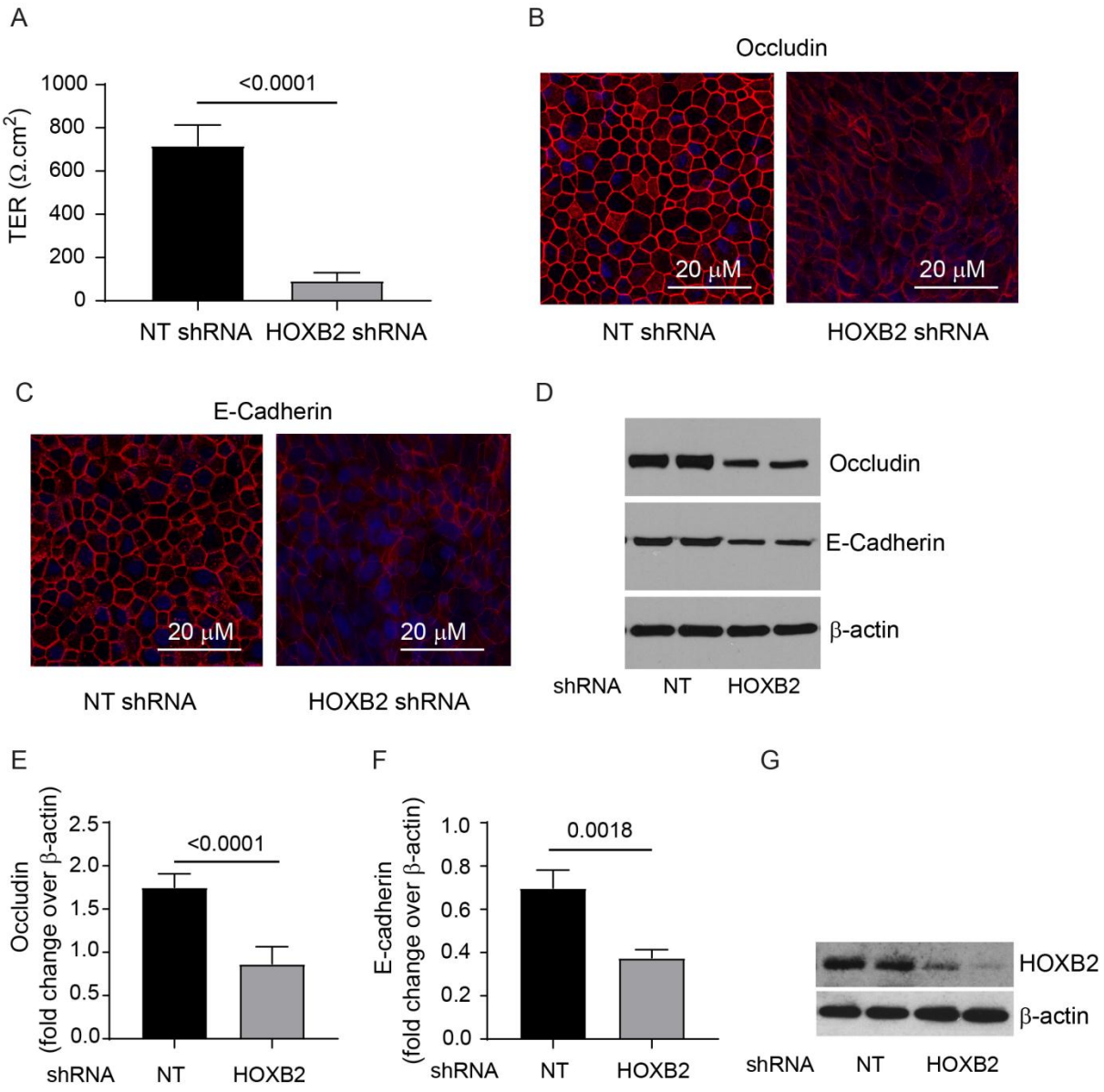
A
1000
800
600
400
200
0
TER (Ω.cm²)
<0.0001
NT shRNA
HOXB2 shRNA
B
Occludin
20 μM
20 μM
NT shRNA
HOXB2 shRNA
C
E-Cadherin
20 μM
20 μM
NT shRNA
HOXB2 shRNA
D
Occludin
E-Cadherin
β-actin
shRNA
NT
HOXB2
E
Occludin
(fold change over β-actin)
2.5
2.0
1.5
1.0
0.5
0.0
<0.0001
shRNA
NT
HOXB2
F
E-cadherin
(fold change over β-actin)
1.0
0.8
0.6
0.4
0.2
0.0
0.0018
shRNA
NT
HOXB2
G
HOXB2
β-actin
shRNA
NT
HOXB2

Figure 7

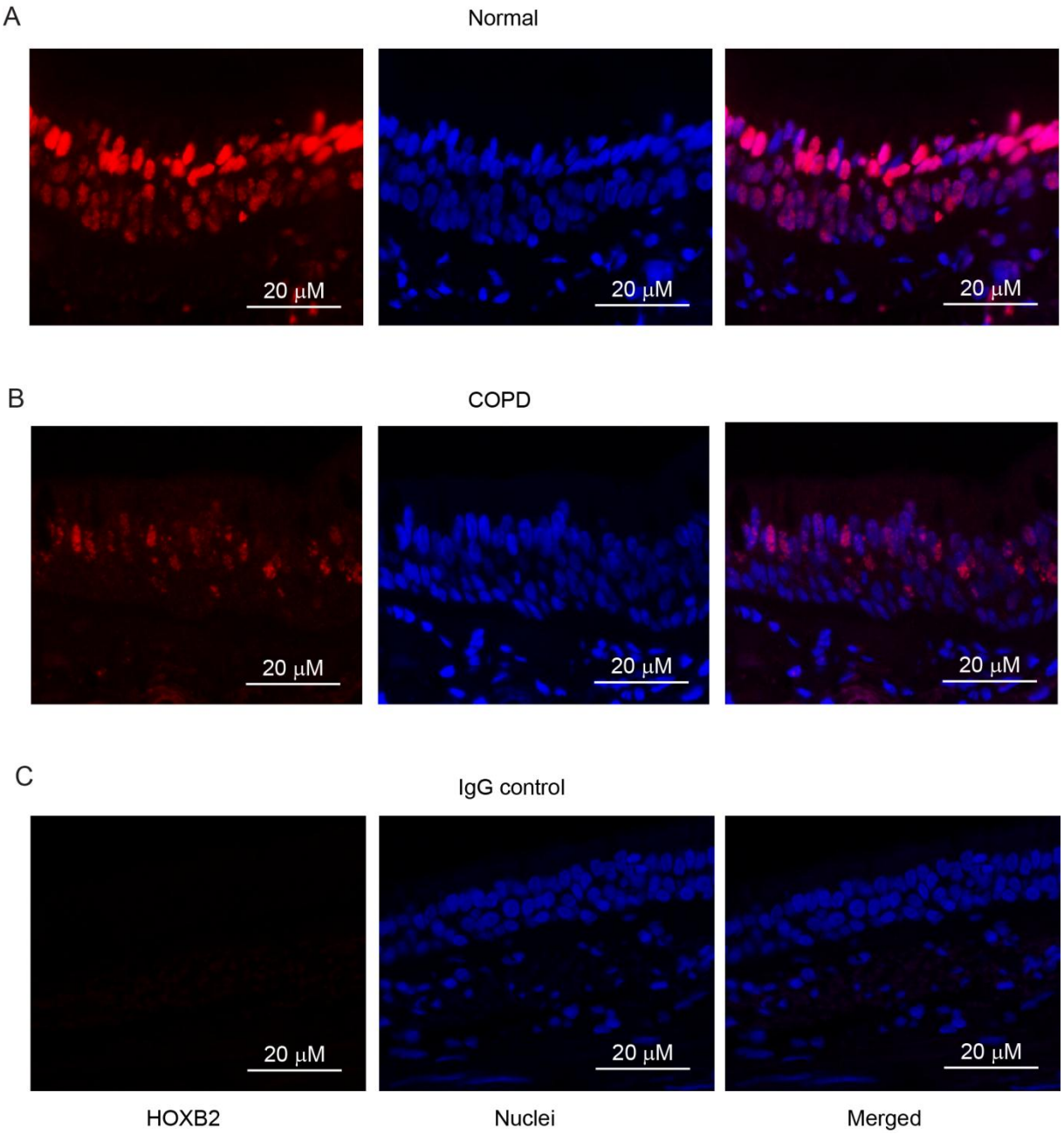
A
Normal
20 μM
20 μM
20 μM
B
COPD
20 μM
20 μM
20 μM
C
IgG control
20 μM
20 μM
20 μM
HOXB2
Nuclei
Merged

Supplemental File

Microarray analysis identifies defect in regenerative and immune response pathways in COPD airway basal cells

Fanny Pineau[1], Gabriella Shumyatsky[1], Nicole Owuor[1], Nisha Nalamala[1], Sudhir Kotnala[1], Sudhir Bolla[1], Nathaniel Marchetti[1], Steven Kelsen[1], Gerard J Criner[1], Uma S Sajjan[1,2*]

Materials and methods

Airway epithelial cells

Basal cells were isolated from bronchial segments of normal donor lungs and explanted lungs from COPD patients at the time of lung transplantation as described previously (1, 2). Collection of the tissue was approved by Institutional Review Board of University Michigan, Ann Arbor, MI and Temple University, Philadelphia. For microarrays analysis tissue was collected from 8 healthy non-smokers and 8 COPD patients who had stopped smoking for at six months at the time of tissue collection. The basal cells were cultured in 12 mm transwells, as described previously (2, 3). Briefly, basal cells were cultured in collagen-coated 10 cm dishes in Bronchial Life medium (LifeLine Cell Technologies, Frederick, MD) until 80% confluent. Cells were harvested, flow-sorted based on the expression of nerve growth factor receptor (NGFR) to isolate basal cells. These cells were seeded in transwells at a density of 1 x 10^5/well. Cells were grown under submerged conditions in Bronchial Life medium until confluent (5 to 7 days) and then maintained at air/liquid interface (ALI) for another 4 weeks to promote mucociliary differentiation. Cells were harvested either at a subconfluent stage that is 3-4 days after seeding (basal cells) or after four weeks of culturing at ALI (Mucociliary-differentiated cell cultures).

16HBE14o- human bronchial epithelial cells are immortalized normal bronchial cells. Cells were grown in Minimum Essential Medium (MEM) supplemented with 10% heatinactivated fetal bovine serum (FBS), and 2 mM of L-glutamine as described (4). Briefly cells were grownin Tranwells and fed from both the basolateral and apical sides and these cells polarize and show transepithelial resistance of 800 to 1000 $\Omega.cm^2$ within 3 to 4 days.

Transfection of airway epithelial cells

16HBE14o- cells were grown in transwells until they reached 90% confluency. Cells were then transfected with non-targeting or HOXB2 siRNA using siRNAmax Lipofectamine (ThermoFisher Scientific, Waltham, MA) and incubated for 6 hours as described previously (5). The transfection medium was replaced with fresh cell culture medium and incubation continued for another 2 days.

RNA and microarray processing

Cells were washed once with PBS, lysed in TRIZOL and total RNA was isolated by using miRNeasy kit (Qiagen, Valencia, CA) involving DNAse treatment step. The quality and concentration of each RNA samples was assessed with Agilent Bioanalyzer (Agilent Technologies, Palo Alto, CA). Biotinylated cDNAs were prepared according to the Affymetrix Plus WT kit protocol (GeneChip® WT Plus Reagent Kit Manual P/N 703174 Rev. 2) from 400 ng total RNA and hybridized to Human Gene 2.1 ST arrays at 48°C. The arrays were washed, stained and scanned using the Affymetrix GeneTitan system (software version 4.3.0.1592). The LIMMA (Linear Models for Microarray Data) methodology was applied to the $\log_2$-transformed expression data to identify differentially expressed genes (DEG) for each comparison. Differentially expressed genes were identified based on statistical significance (p-value of < 0.05 and up/down regulated by more than 2-fold) and further analyzed. Normalized data and raw data are available in Gene Expression Omnibus (GEO) with accession number GSE137557.

Gene Ontology

Gene Ontology (GO) and KEGG pathways were analyzed with WebGestalt (WEB-based GEne SeT AnaLysis Toolkit) (6) using the Benjamini-Hochberg correction for multiple testing (FDR 5%). For Gene Ontology, only Biological Process terms are discussed because Cellular Component and Molecular Function terms were less relevant.

Flow cytometry

Mucociliary-differentiated cells were dissociated with accutase (ThermoFisher Scientific, Waltham. MA), cells were fixed with 4% paraformaldehyde, and incubated in PBS containing 1% BSA and 0.5% saponin to permeabilize and block the cells simultaneously. Cells were then incubated with acetylated tubulin (Sigma Aldrich, St. louis, MO), Muc5AC (Abcam, Cambridge, MA) or TP63 (Abcam), bound antibodies were detected by using Alexafluor-labeled second antibodies. The cells were then analyzed in FACSCalibur Flow cytometer (BD Biosciences, San Jose, CA). The data was analyzed by FlowJo version 10 (Tree Star, Ashland, OR).

Transepithelial resistance

Transepithelial resistance of airway epithelial cell cultures maintained at air/liquid interface (ALI) for two weeks or 16HBE14o- cells cultured in transwells for 4 days was determined by using EVOM volt/Ohm meter (World precision Instruments, Sarasota, FL) with EnOhm chambers as previously described (4).

Histology

For histological evaluation, cell cultures were fixed in buffered formalin, embedded in paraffin, 5 µ thick sections were deparaffinized and stained with hematoxylin and eosin (H and E) or periodic acid Schiff's (PAS) reagent (1).

Real-time PCR

cDNAs were synthesized from 500 ng of total RNA using LunaScript RT SuperMix kit (New England Biolabs, Ipswich, MA). Expression of *ADAMTSL3*, *ELF5*, *HOXA1*, *HOXB2*, *IVL*,

KRTDAP, *STC2, ELF5, VGLL1, MUC5AC and FOXJ1* was determined by using a primetime probe based realtime PCR assays (Integrated DNA Technologies, Coralville, IA). The expression levels of each gene is presented as fold change over house-keeping gene, glyceraldehyde 3-phosphate dehydrogenase (*GAPDH*).

Immunofluorescence staining of cell cultures and lung sections.

Cells growing in the transwells were washed with PBS and fixed in ice cold methanol at 5 min (for occludin) or in 4% paraformaldehyde followed by permeabilization with 0.1% Triton X-100 in PBS for 15 min (for E-cadherin) (4, 5, 7). The cells were then blocked with 1% BSA and incubated in 1:50 (for E-cadherin) or 1:100 (for occludin) (both antibodies are purchased from ThermoFisher Scientific) overnight at 4° C. The bound antibody was detected by using appropriate Alexafluor-conjugated second antibodies, counter stained with DAPI to visualize nuclei and imaged under Zeiss Confocal microscope.

Lung tissue at second and third branching of bronchi was collected from 6 COPD and 6 healthy non-smokers under the approval of Temple Institute Review Board. All the COPD subjects were at end stage disease and undergoing lung transplantation. The tissues were fixed in 10% buffered formaldehyde and embedded in paraffin. Five micron thick lung sections were deparaffinized, subjected to antigen retrieval by boiling in sodium citrate buffer and endogenous peroxidase activity was quenched with hydrogen peroxide. The sections were permeabilized with 0.3% TRITON X-100, blocked with 5% normal horse serum and incubated with HOXB2 antibody (Developmental Studies Hybridoma Bank, University of Iowa, Iowa City, IA) for 16 h at 4°C. Unbound antibody was removed, washed and then incubated with a second antibody conjugated with HRP (ImmPRESS HRP anti-mouse or anti-rabbit IgG, Vector Laboratories, Burlingame,

CA). Sections were then incubated with tyramide conjugated with Alexa Flour 488 (Thermo Fisher Scientific), counter stained with DAPI and imaged using a fluorescence microscope.

Western blot analysis

After relevant treatment, cells were washed with cold PBS and lysed in RIPA buffer containing protease and phosphatase inhibitors. Equal amount of protein was subjected to Western blot analysis with antibodies to E-cadherin (abcam), occludin (BD Biosciences), HOXB2 or β-actin (Sigma Aldrich). Specific bands were quantified by densitometry using NIH image J and expressed as fold change over β-actin or over respective total protein.

Statistical analysis

To validate the DEGs identified by microarray analysis cells obtained from 8 normal and 8 COPD subjects were used in most of the experiments. The data was expressed as median with range and the statistical significance was assessed by non-parametric analysis, Mann-Whitney test to compare two groups and ANOVA on Ranks with Kruskal Wallace non parametric test to compare three groups. Other experiments were repeated at least 3 times in duplicates and the data presented as mean ± SD and statistical significance was assessed by unpaired t test. A p-value of ≤ 0.05 was considered as statistically significant.

References

1. Schneider D, Ganesan S, Comstock AT, Meldrum CA, Mahidhara R, Goldsmith AM, Curtis JL, Martinez FJ, Hershenson MB, Sajjan U. Increased cytokine response of rhinovirus-infected airway epithelial cells in chronic obstructive pulmonary disease. *American journal of respiratory and critical care medicine* 2010; 182: 332-340.

2. Jing Y, Gimenes JA, Mishra R, Pham D, Comstock AT, Yu D, Sajjan U. NOTCH3 contributes to rhinovirus-induced goblet cell hyperplasia in COPD airway epithelial cells. *Thorax* 2019; 74: 18-32.

3. Ganesan S, Pham D, Jing Y, Farazuddin M, Hudy MH, Unger B, Comstock AT, Proud D, Lauring AS, Sajjan US. TLR2 Activation Limits Rhinovirus-Stimulated CXCL-10 by Attenuating IRAK-1-Dependent IL-33 Receptor Signaling in Human Bronchial Epithelial Cells. *Journal of immunology* 2016; 197: 2409-2420.

4. Sajjan U, Wang Q, Zhao Y, Gruenert DC, Hershenson MB. Rhinovirus disrupts the barrier function of polarized airway epithelial cells. *American journal of respiratory and critical care medicine* 2008; 178: 1271-1281.

5. Unger BL, Ganesan S, Comstock AT, Faris AN, Hershenson MB, Sajjan US. Nod-like receptor X-1 is required for rhinovirus-induced barrier dysfunction in airway epithelial cells. *J Virol* 2014; 88: 3705-3718.

6. Wang J, Vasaikar S, Shi Z, Greer M, Zhang B. WebGestalt 2017: a more comprehensive, powerful, flexible and interactive gene set enrichment analysis toolkit. *Nucleic acids research* 2017; 45: W130-W137.

7. Faris AN, Ganesan S, Chattoraj A, Chattoraj SS, Comstock AT, Unger BL, Hershenson MB, Sajjan US. Rhinovirus Delays Cell Repolarization in a Model of Injured/Regenerating

Human Airway Epithelium. *American journal of respiratory cell and molecular biology* 2016; 55: 487-499.

Figure Legends

Supplemental Figure 1. Correlation of tissue developmental genes with polarization and differentiation markers. Total RNA or protein was extracted from 8 normal and 8 COPD patients at 1 (basal cells), 3 (polarized cells) and 5 (differentiated cells) weeks of culturing. mRNA expression of ELF5, VGLL1 and KRTDAP was assessed in basal cells and correlated with the expression of MUC5AC and FOXJ1 mRNA in differentiated cells (A and B). TER was determined at 3 weeks of culturing and corrleated with the expression of ELF5, VGLL1 and KRTDAP. Data represents median with range form 8 COPD and 8 normal subjects and statistical significance was determined by Mann-Whitney test.

Supplemental Table 1. Study population

Cells used for microarrays

Subject	Age	Sex	Pack-years	FEV1% predicted
Normal (8)	**50**	**4:4**		
N4	59	F	-	-
N17	33	M	-	-
N18	16	M	-	-
N19	50	F	-	-
N20	52	M	-	-
N22	62	M	-	-
N24	50	F	-	-
N27	48	F	-	-
COPD (8)	**54**	**5:3**	**41.25**	**17**
C6	49	F	25	17
C10	53	F	37.5	14
C11	59	M	70	22
C12	49	F	136	13
C14	55	M	25	17
C15	45	M	31.25	17
C18	67	M	90	20
C19	64	M	45	29

Tissues used for immunohistochemistry

Normal (4)				
1201	70	M	-	-
1220	67	M	-	-
1283	47	F	-	-
1316	67	F	-	-
COPD (4)				
713	73	M	N/A	21
1193	58	F	N/A	43
1209	75	M	N/A	22
1213	59	F	N/A	18

N/A: Not available

Supplementary Table 1. Differentially expressed probes between COPD and normal basal cells

ID	C Avg (log2	N Avg (log C	Standard	N Standard	Fold Chan	P-val	FDR P-val	Public Gen	Gene Symbo	Description	Chromoso	Strand	Start	Stop
17056098	1.51	3.67	0.7	0.5	-4.47	1.79E-06	0.0496	NM_0055:	**HOXA1**	homeobox A1	chr7	-	27132612	27135625
16678496	4.92	3.78	0.41	0.38	2.21	2.06E-06	0.0496	NM_1750!	**HIST3H2BB**	histone cluster 3, H2bb	chr1	+	2.29E+08	2.29E+08
16991948	6.98	8.13	0.45	0.28	-2.21	3.28E-06	0.0527	NM_0010!	**TENM2**	teneurin transmembrane protein	chr5	+	1.67E+08	1.68E+08
17023799	2.93	4.61	0.57	0.65	-3.19	2.02E-05	0.0814	NM_1451:	**SLC2A12**	solute carrier family 2 (facilitated	chr6	-	1.34E+08	1.34E+08
17085190	3.37	1.98	0.57	0.44	2.63	2.05E-05	0.0814				chr9	+	42037464	42037558
17085457	3.37	1.98	0.57	0.44	2.63	2.05E-05	0.0814				chr9	+	67864533	67864627
17094376	3.37	1.98	0.57	0.44	2.63	2.05E-05	0.0814				chr9	-	46669492	46669586
17107309	5.06	6.67	0.61	0.57	-3.05	4.72E-05	0.1382	NM_0162(	**VGLL1**	vestigial-like family member 1	chrX	+	1.36E+08	1.36E+08
16820820	5.12	4.08	0.28	0.48	2.05	0.0001	0.1557	NR_00307	**SNORD111**	small nucleolar RNA, C/D box 11:	chr16	+	70571908	70572001
16913627	1.75	3.21	0.51	0.72	-2.76	0.0001	0.1557	NM_0011(	**ARHGAP40**	Rho GTPase activating protein 4(	chr20	+	37230577	37279678
17100201	5.23	6.48	0.59	0.66	-2.38	0.0002	0.1636	NM_0046(	**CLIC3**	chloride intracellular channel 3	chr9	-	1.4E+08	1.4E+08
16846218	1.89	3.29	0.31	0.93	-2.64	0.0002	0.1661	NM_0021-	**HOXB2**	homeobox B2	chr17	-	46618256	46623441
17121722	8	9.26	0.46	0.71	-2.39	0.0002	0.183				TCONS_l2_	+	1	1201
16980051	3.83	2.19	0.8	0.5	3.12	0.0003	0.2061	NM_0011:	**CLGN**	calmegin	chr4	-	1.41E+08	1.41E+08
16884607	2.76	3.76	0.45	0.69	-2	0.0003	0.2065	NM_0122'	**IL36RN**	interleukin 36 receptor antagonis	chr2	+	1.14E+08	1.14E+08
17016509	5.33	4.08	0.44	0.58	2.39	0.0003	0.2065	ENST0000(	**HIST1H3J**	histone cluster 1, H3j	chr6	-	27858093	27858588
16734355	2.59	3.99	0.63	0.88	-2.64	0.0003	0.2099	NR_00219	**H19; MIR675**	H19, imprinted maternally expre	chr11	-	2016406	2022700
17016366	6.02	4.51	0.61	0.51	2.84	0.0004	0.2109	NM_0035:	**HIST1H2AB**	histone cluster 1, H2ab	chr6	-	26033320	26033796
16660014	3.31	4.76	0.63	0.76	-2.73	0.0005	0.2358	NM_0133!	**PADI1**	peptidyl arginine deiminase, type	chr1	+	17531621	17572501
16760953	4.49	6.31	0.68	0.85	-3.53	0.0005	0.2506	NM_0012!	**MFAP5**	microfibrillar associated protein	chr12	-	8789942	8815484
16671514	1.21	2.84	0.53	0.84	-3.08	0.0007	0.2558	NR_03621	**MIR4258**	microRNA 4258	chr1	+	1.55E+08	1.55E+08
17121866	6.69	8.05	0.51	0.84	-2.57	0.0008	0.2692				TCONS_l2_	+	1	1829
16773260	5.06	7.23	1.26	1.4	-4.48	0.0008	0.2692	NM_0011!	**ATP12A**	ATPase, H+/K+ transporting, non	chr13	+	25254549	25285923
16873528	1.14	2.27	0.49	0.66	-2.19	0.0009	0.2692	XR_24400:	**LOC645553**	uncharacterized LOC645553	chr19	-	46692287	46706319
16669278	2.21	3.23	0.4	0.6	-2.02	0.0009	0.2747	NM_0177(	**FAM46C**	family with sequence similarity 4	chr1	+	1.18E+08	1.18E+08
16882834	4.2	6.31	0.73	1.75	-4.32	0.001	0.2747	NM_0023'	**MAL**	mal, T-cell differentiation protein	chr2	+	95691422	95719737
16874683	4.47	5.9	0.77	0.84	-2.68	0.0011	0.2797	NM_0010'	**KLK5**	kallikrein related peptidase 5	chr19	-	51446559	51456344
16746217	1.13	2.27	0.52	1.16	-2.2	0.0011	0.2815				chr11	-	1.3E+08	1.31E+08
16730157	1.25	2.59	0.31	1.16	-2.53	0.0011	0.2887	NM_0010!	**HEPHL1**	hephaestin-like 1	chr11	+	93754378	93847374
17044485	2.04	3.06	0.63	0.25	-2.04	0.0012	0.294	NR_03836	**HOTAIRM1**	HOXA transcript antisense RNA,	chr7	+	27135266	27139877
16842403	4.86	6.43	0.62	0.79	-2.97	0.0012	0.2981	NM_0010-	**LGALS9B**	lectin, galactoside-binding, solub	chr17	-	20352708	20372296
17122712	3.18	4.29	0.55	0.39	-2.15	0.0016	0.3226				TCONS_l2_	+	1	507
16737282	3.84	4.92	0.57	0.93	-2.12	0.0022	0.3422	NM_0012-	**ELF5**	E74-like factor 5 (ets domain tra	chr11	-	34499855	34535352
16874702	7.42	8.45	0.5	0.93	-2.05	0.0024	0.3483	NM_0012(	**KLK7**	kallikrein related peptidase 7	chr19	-	51479729	51487320
16816962	3.45	4.65	0.72	0.6	-2.31	0.0027	0.3578	NM_0010:	**SCNN1G**	sodium channel, non voltage gat	chr16	+	23194036	23228204
16861126	1.96	3.94	0.55	1.93	-3.96	0.0028	0.3578	NM_0012!	**UPK1A**	uroplakin 1A	chr19	+	36157715	36169367
17108856	6.59	4.99	0.6	1.52	3.03	0.003	0.3578	XR_92127(	**LOC1019301**	zinc finger protein 839-like	chrX	-	3771051	3804591
16765080	6.28	7.86	1.1	0.94	-2.99	0.0031	0.3578	NM_0022'	**KRT4**	keratin 4, type II	chr12	-	53200327	53208335
16735727	1.19	2.33	0.47	0.84	-2.21	0.0031	0.3578				chr11	-	9865362	9865423
17121738	5.31	6.36	0.63	0.65	-2.06	0.0032	0.3589				TCONS_l2_	+	1	1110
16671061	1.39	2.96	0.52	1.24	-2.96	0.0038	0.3693	NM_0010'	**KPRP**	keratinocyte proline-rich protein	chr1	+	1.53E+08	1.53E+08
17125596	6.98	5.6	0.41	1.24	2.6	0.0039	0.3693				TCONS_l2_	+	1	318
16764907	0.89	2	0.63	0.85	-2.16	0.0039	0.3693	NM_1730!	**KRT6C**	keratin 6C, type II	chr12	-	52862300	52867569
16972229	6.24	4.24	1.33	1.16	3.99	0.004	0.3693	NM_0071!	**ANXA10**	annexin A10	chr4	+	1.69E+08	1.69E+08
16693393	3.14	4.44	0.95	0.91	-2.46	0.0042	0.3693	NM_0203!	**PGLYRP4**	peptidoglycan recognition protei	chr1	-	1.53E+08	1.53E+08
16966621	4.67	5.87	0.78	1.06	-2.29	0.0043	0.3726	NM_0012!	**CWH43**	cell wall biogenesis 43 C-termina	chr4	+	48988264	49064098
16711390	0.98	2.09	0.36	0.94	-2.15	0.0048	0.3794	NM_0174'	**CALML5**	calmodulin-like 5	chr10	-	5540658	5541533
17002429	4	5.12	1.28	0.81	-2.18	0.005	0.3843	NM_0251!	**ATP10B**	ATPase, class V, type 10B	chr5	-	1.6E+08	1.6E+08
16871403	4.83	6.29	1.26	1.64	-2.74	0.0054	0.3865	NM_0011(	**SBSN**	suprabasin	chr19	-	36014269	36019253
17121736	3.89	5.13	0.67	0.97	-2.37	0.0059	0.3939				TCONS_l2_	+	1	2334
17005862	2.7	1.62	0.26	0.83	2.13	0.006	0.3939	NM_0035:	**HIST1H3H**	histone cluster 1, H3h	chr6	+	27777842	27778314
16872777	4.43	6.56	1.09	2.27	-4.39	0.007	0.4035	NM_0324!	**CNFN**	cornifelin	chr19	-	42891171	42894444
16874751	3.03	5.24	0.98	2.05	-4.65	0.0071	0.4035	NM_0195!	**KLK12**	kallikrein related peptidase 12	chr19	-	51532348	51538486
17125236	3.7	2.38	1	0.84	2.5	0.0078	0.4138				TCONS_l2_	+	1	397
17125594	6.53	5.33	0.52	1.09	2.3	0.0081	0.4138				TCONS_l2_	+	1	412
17079346	3.74	4.77	0.68	0.51	-2.04	0.0086	0.4144				chr8	-	96691066	96691143
17119706	3.74	4.77	0.68	0.51	-2.04	0.0086	0.4144				tc5302189	+	1	78
16671094	3.92	5.1	1.03	1.1	-2.27	0.0093	0.4179	NM_0055-	**IVL**	involucrin	chr1	+	1.53E+08	1.53E+08
16959505	1.71	0.71	0.7	0.65	2.01	0.01	0.4261				chr3	-	1.35E+08	1.35E+08
16671023	5.35	7.13	1.09	1.7	-3.43	0.0112	0.4363	NM_0190(	**CRCT1**	cysteine rich C-terminal 1	chr1	+	1.52E+08	1.52E+08
16871349	2.47	3.59	0.6	1.57	-2.17	0.0114	0.4387	NM_0012-	**KRTDAP**	keratinocyte differentiation-asso	chr19	-	35978226	35986460
16799739	6.73	4.83	1.32	0.45	3.72	0.0118	0.4445	NM_0011-	**CHAC1**	ChaC glutathione-specific gamma	chr15	+	41244055	41248717
16670681	2.16	3.21	0.49	1.02	-2.06	0.0119	0.446	NM_0035(	**ANXA9**	annexin A9	chr1	+	1.51E+08	1.51E+08
16840799	2.32	4.46	1.27	1.49	-4.41	0.0125	0.4492	NM_0011!	**ALOX12B**	arachidonate 12-lipoxygenase, 1	chr17	-	7975954	7991022
17094586	3.77	2.71	0.9	0.89	2.1	0.0127	0.4527				chr9	-	69821760	69821841
16693383	3.18	4.21	0.95	0.95	-2.03	0.0134	0.4584	NM_0528!	**PGLYRP3**	peptidoglycan recognition protei	chr1	-	1.53E+08	1.53E+08
16874722	2.66	3.77	0.6	0.9	-2.15	0.0136	0.4592	NM_0123'	**KLK9; KLK8**	kallikrein related peptidase 9; ka	chr19	-	51505664	51512890
16743593	4.66	6.05	1.69	0.99	-2.62	0.0141	0.462	NM_0046'	**TRPC6**	transient receptor potential catio	chr11	-	1.01E+08	1.02E+08
16949261	3.18	2.17	0.44	0.54	2.01	0.0143	0.4631				chr3	+	1.86E+08	1.86E+08
17055551	2.73	1.72	0.74	0.47	2.01	0.0156	0.4695	NR_11001	**LOC1019276**	uncharacterized LOC101927630	chr7	-	17503069	17598533
17079293	5.67	4.62	0.75	0.29	2.07	0.0157	0.4695	NM_0577-	**CCNE2**	cyclin E2	chr8	-	95891998	95908906
17044253	4.05	5.18	1.27	0.65	-2.2	0.0157	0.4695	NM_0010(	**GPNMB**	glycoprotein (transmembrane) n	chr7	+	23275586	23314729
16733068	2.86	1.72	1.17	0.68	2.21	0.016	0.4734				chr11	+	1.25E+08	1.25E+08
16660038	3.26	5.08	1.03	0.9	-3.55	0.0168	0.4812	NM_0162:	**PADI3**	peptidyl arginine deiminase, type	chr1	+	17575593	17610728
16888510	1.09	2.34	0.67	1.03	-2.38	0.0185	0.4929				chr2	+	1.87E+08	1.87E+08
16693427	1.82	3.17	0.89	1.18	-2.55	0.0186	0.4929	NM_0029(	**S100A7**	S100 calcium binding protein A7	chr1	-	1.53E+08	1.53E+08
16841634	2.31	3.41	0.96	0.55	-2.14	0.0193	0.4949	NM_0012!	**CDRT1**	CMT1A duplicated region transcr	chr17	-	15468797	15523018
16831890	3.56	4.81	0.74	0.89	-2.37	0.0206	0.5014	NM_0010-	**LGALS9C**	lectin, galactoside-binding, solub	chr17	+	18380098	18398259
17124674	2.79	1.63	0.88	0.53	2.23	0.0214	0.5068				TCONS_l2_	+	1	306

17125110	4.08	3	1.21	0.38	2.12	0.0224	0.5127			TCONS_l2_	+	1	381	
17000168	6.85	8.07	1.32	0.26	-2.33	0.0228	0.5133	NM_0048{	**CXCL14**	chemokine (C-X-C motif) ligand 1	chr5	-	1.35E+08	1.35E+08
16947041	2.47	1.27	1.28	0.69	2.3	0.0228	0.5133	XR_92458!	**LOC1053741**	uncharacterized LOC105374160	chr3	+	1.52E+08	1.52E+08
16936033	5.23	4.2	0.65	0.44	2.04	0.024	0.5166				chr22	-	46020411	46020512
16844419	1.66	3.28	0.94	1.15	-3.06	0.0241	0.5175	NM_0190:	**KRT24**	keratin 24, type I	chr17	-	38854243	38860002
17012709	8.65	9.82	0.57	0.55	-2.25	0.0262	0.5271	NR_00243	**SNORD100; S**	small nucleolar RNA, C/D box 10(	chr6	+	1.33E+08	1.33E+08
16972291	1.96	3.04	1.13	1.12	-2.11	0.0263	0.5271				chr4	+	1.7E+08	1.7E+08
16997010	1.75	0.65	1.09	0.62	2.15	0.0327	0.5487	OTTHUMT	**GTF2H2**	general transcription factor IIH s	chr5	-	70328995	70330227
16761693	3.68	4.94	1.19	1.29	-2.39	0.0351	0.5562	NR_03655	**LINC01559**	long intergenic non-protein codi	chr12	-	13523605	13540101
17025738	0.94	2.02	0.66	2.29	-2.11	0.036	0.5609	NR_11709	**LOC441178;**	uncharacterized LOC441178; unc	chr6	-	1.68E+08	1.68E+08
16804106	4.25	3.15	0.95	0.84	2.14	0.0364	0.5629	NM_0013(	**ADAMTSL3**	ADAMTS like 3	chr15	+	84322838	84708594
17126218	2.93	4.77	0.83	1.39	-3.57	0.0372	0.5642				CDR1_AS	+	1	1487
17122142	3.67	5.05	1.75	1.24	-2.59	0.0392	0.568				TCONS_l2_	+	1	241
16990862	5.63	6.67	1.25	0.82	-2.05	0.0406	0.5749	NM_0013(	**ABLIM3**	actin binding LIM protein family,	chr5	+	1.49E+08	1.49E+08
16851708	2.64	4.32	1.65	1.96	-3.21	0.0411	0.5771	NM_0019/	**DSG1**	desmoglein 1	chr18	+	28898052	28937394
17038059	2.96	1.38	1.23	1.19	3	0.0431	0.5834				chr6_qbl_l	+	2661007	2677562
17121790	1.83	0.78	1.22	0.48	2.08	0.0446	0.5871				TCONS_l2_	+	1	2289
17125866	0.85	1.98	0.79	1.09	-2.19	0.0471	0.596				gi3011733	+	1	77
16829801	1.97	3	0.75	1.15	-2.04	0.0474	0.5961	NM_0011:	**SPNS2**	spinster homolog 2 (Drosophila)	chr17	+	4402129	4443228
17002898	6.63	5.19	1.25	0.56	2.72	0.0488	0.5965	NM_0037:	**STC2**	stanniocalcin 2	chr5	-	1.73E+08	1.73E+08

Supplemental Table 3. Biological Process terms enriched in COPD vs normal basal cells

GeneSet	description	size	overlap	expect	enrichmentRatio	FDR p-value
GO:0008544	epidermis development	437	11	1.2	8.8	2.5E-04
GO:0019730	antimicrobial humoral response	106	6	0.3	19.9	1.6E-03
GO:0070268	cornification	106	6	0.3	19.9	1.6E-03
GO:0030216	keratinocyte differentiation	280	8	0.8	10.0	1.9E-03
GO:0061844	antimicrobial humoral immune response mediated by antimicrobial peptide	65	5	0.2	27.0	1.9E-03
GO:0043588	skin development	390	9	1.1	8.1	1.9E-03
GO:0031424	keratinization	210	7	0.6	11.7	2.5E-03
GO:0009913	epidermal cell differentiation	331	8	0.9	8.5	3.9E-03
GO:0006959	humoral immune response	233	7	0.7	10.5	3.9E-03
GO:0030855	epithelial cell differentiation	712	10	2.0	4.9	2.1E-02
GO:0009888	tissue development	1839	16	5.2	3.1	2.1E-02
GO:0002325	natural killer cell differentiation involved in immune response	5	2	0	140.4	4.7E-02
GO:0032826	regulation of natural killer cell differentiation involved in immune response	5	2	0	140.4	4.7E-02
GO:0018101	protein citrullination	5	2	0	140.4	4.7E-02
GO:0036414	histone citrullination	5	2	0	140.4	4.7E-02

Supplemental Figure 1